

**Development of Small Scale Soft X-ray Lasers;
Aspects of Data Interpretation.**

C.H. Skinner, D. Kim, D.Voorhees, and S. Suckewer[†]

*Princeton University Plasma Physics Laboratory,
Princeton, N.J. 08543*

ABSTRACT

The widespread application of soft x-ray laser technology is contingent on the development of small scale soft x-ray lasers that do not require large laser facilities. Progress in the development of soft x-ray lasers pumped by a Nd laser of energy 6-12J is reported below. Some aspects of data interpretation and gain measurements in such systems are discussed.

DISCLAIMER

This report was prepared as an account of work sponsored by an agency of the United States Government. Neither the United States Government nor any agency thereof, nor any of their employees, makes any warranty, express or implied, or assumes any legal liability or responsibility for the accuracy, completeness, or usefulness of any information, apparatus, product, or process disclosed, or represents that its use would not infringe privately owned rights. Reference herein to any specific commercial product, process, or service by trade name, trademark, manufacturer, or otherwise does not necessarily constitute or imply its endorsement, recommendation, or favoring by the United States Government or any agency thereof. The views and opinions of authors expressed herein do not necessarily state or reflect those of the United States Government or any agency thereof.

[†] also at Mechanical and Aerospace Engineering Dept., Princeton University

1. INTRODUCTION

The field of x-ray laser technology has recently matured to the stage where the application of these devices to fields such as x-ray microscopy is underway¹ and commercial units are being planned with a view to industrial applications such as microlithography. A critical factor in such development is the scale and hence cost of these devices. The collisionally pumped soft x-ray laser in neon-like ions, developed at Livermore², requires a large scale laser facility such as Novette or Nova to create a plasma of appropriate conditions. A 3mJ, 182Å soft x-ray laser based on a recombining plasma was developed at Princeton³ with an efficiency almost 2 orders of magnitude higher than the collisionally pumped case. However the pump laser required, a 300J CO₂ laser, was still large. In order to increase the output energy and efficiency of the 182Å soft x-ray laser we have been developing soft x-ray amplifiers. A gain of 8cm⁻¹ has been measured in a 3mm long carbon plasma transversely pumped by a 3nsec Nd laser pulse of energy 25J, of which only 15J impinged on the target⁴. We have also demonstrated amplification of 4.5 cm⁻¹ in a plasma pumped by only 6J⁵. In this paper we will present the initial gain measurements at 182Å in a carbon plasma pumped by a 6J laser pulse. We will also present some measurements showing a non-linear rise of intensity with length in an Al plasma pumped by a 6 or 12J laser pulse. We will discuss aspects of data interpretation and gain measurement in such systems.

2. AMPLIFICATION AT 182Å WITH A 6J PUMP LASER

In this section, we present gain measurements on the CVI 182Å transition in a carbon plasma produced with a 6J, 3 nsec Nd:glass laser pulse. The experimental set-up was the same as presented in an earlier paper⁴.

Figure 1 shows the rotatable target system used . A 67-cm focal-length spherical lens and 450 cm focal length cylindrical lens were operated in a slightly defocussed arrangement to produce a $\sim 200 \mu\text{m} \times 5 \text{ mm}$ line-focus on a length-varying cylindrical target. The target lengths used in this experiment were 1, 2.5, and 4.5 mm (limited by the diameter of the access ports in the target chamber). A $0.8 \times 2 \text{ mm}$ slot in a mask located 1.5 cm away from the target in the axial direction, selected a limited spatial region which was viewed by an axial soft x-ray spectrometer equipped with a multichannel detector. In the experiments the slot was placed in such a way that it selected a spatial region 0.0 - 0.8 mm from the target surface.

Figure 2 shows the intensity variation of the CV 135Å, OVI 173Å, CVI 182Å, and CV 186Å lines with respect to the plasma length using a 6J, 3 nsec. laser pulse. No stainless steel blade or magnetic field was used. The CVI 182Å line (3-2 transition) increased non-linearly while the CVI 135Å (4-2 transition) and some other lines increased linearly as expected from optically thin spontaneous emission from a homogeneous plasma of length equal to the length of the target. This was a clear indication of gain on the 182Å line. The difference in the length dependence of the 182Å and 135Å lines here is very important (the contribution of the 4th order of the CVI 33.74Å line to 135Å, even for the 1mm plasma, was negligible due to the large opacity of this line). The data were fitted by a nonlinear regression model⁶ which performed a least-square fit of the data to the relation:

$$I(L) = \frac{(\exp(GL) - 1)^{3/2}}{(GL \times \exp(GL))^{1/2}} \quad (1).$$

This describes the output intensity of a Doppler-broadened, homogeneous source of amplified spontaneous emission of gain-length product GL. The fit yielded a value of the gain of 4.5 / cm on the CVI 182Å line and of 0.5 / cm on the CVI 135 Å line (see fig. 3). This result augers well for the commercial availability in the near future of relatively inexpensive soft x-ray lasers for a variety of novel applications.

3. EXPERIMENTS ON ALUMINIUM PLASMAS, ASPECTS OF DATA INTERPRETATION

In the above experiment the plasma length was limited to 4.5mm by the internal diameter of the ports available in the target chamber inside the magnet. A new target chamber was constructed in which plasmas of length of 1cm or more could be produced. This system also had much more flexibility for positioning and angular adjustment of the target and detector (Fig. 4). In this section we present some results from this system showing an non-linear increase of intensity with length of AlX and AlXI lines in an aluminum plasma. The lithium sequence ions such as AlXI were first used in soft x-ray laser development by Jaeglé and coworkers⁷, however the present work on aluminium plasmas pumped with a low energy Nd laser was primarily stimulated by the surprising results of Hara et.al.⁸ indicating gain on almost all AlX and AlXI lines observed. It was a simple task to repeat the experiments of Hara et. al. by changing the target material to aluminium.

A Nd glass laser, operated at 6J or 12J, was brought to a line focus by a combination of 4 lenses. Two spherical lenses with a combined focal length of 60cm and two cylindrical lenses produced a sharp line focus 12mm long with a width of 50µm (FWHM) on a rotatable aluminium target with sectors of differing

length (2, 6, 10mm) . Axial emission was detected by a soft X-ray multichannel spectrometer "SOXMOS" ⁹. SOXMOS was attached to a rotatable arm pivoted under the target so that the angle it viewed could be varied by $\pm 2^\circ$ with respect to the target. The target assembly was on a platform that could be rotated $\pm 2^\circ$ around a vertical axis so that by combining the two motions, emission over a $\pm 4^\circ$ axial range in the horizontal plane could be recorded. This system was designed to allow the most precise alignment of the target with respect to the spectrometer and also enable the detection of a stimulated soft X-ray beam that had been deviated from the nominal axial direction by refraction in the plasma. A slot with open area 3mm high and 0.35mm wide was placed on axis 4 cm from the target to limit the view of the spectrometer. The position of the slot could be adjusted to view regions of the plasma at different distances from the target surface.

In the experiment a search for gain was performed by varying the experimental parameters (including the target length) and looking for conditions in which the intensity of candidate lines increased with length at a rate that was faster than linear. A faster-than-linear rise of intensity with length is commonly regarded as conclusive evidence for stimulated emission.

Figure 5 shows axial spectra of AlIV, OVI, AlX, and AlXI lines at 2mm and 10mm target lengths. A dramatic increase of intensity of the AlX and AlXI lines is seen with the 10mm target as compared to 2mm, while the AlIV and OVI lines show a sub-linear increase. Figure 6 shows peak intensities taken at 2, 6, and 10mm target lengths and a curve fit to the data. The theoretical fit was derived from a nonlinear regression model⁶ as in the CVI case. In general the transition linewidth will be a convolution of Stark and Doppler broadening but for the present purposes we have used the gain equation based on the Doppler broadening.

A higher laser energy was used in order to increase the output intensity. Data taken at 12J is shown in Figs. 7 and 8. Here the increase with length is even more dramatic, for instance the ALXI 141Å (3s-4p) intensity increases from 2mm to 10mm by a factor of x50 and is an excellent fit to the gain equation for a gain of $G = 5.1/\text{cm}$. The ALXI 150Å (3p-4d), 154Å (3d-4f) and ALX 177Å (3d-4f) lines also show a length dependence which is a very close fit to the gain equation at comparable values of gain. Similar results were obtained for the ALXI 105.7Å (3d-5f) and 103.8Å (5d-3p) lines.

The emission from the plasma was recorded on a time-resolving streaked spectrometer¹⁰, "TGSS" placed on-axis, on the opposite side of the plasma to the spectrometer: SOXMOS. A free standing gold transmission grating with a 3000Å period and 250µm entrance slit, dispersed the axial plasma emission along the entrance slit of an x-ray streak camera. The entrance slit was 12mm long, 1mm wide, and coated with a 200Å thick aluminium photocathode. This grating, streak camera arrangement resulted in a source-size-limited spectral resolution for these experiments of approximately 3Å. The spectral range of the instrument extended from 110Å to 190Å.

The streaked image was amplified by an image intensifier and recorded on calibrated TriX film placed in contact with the output of the image intensifier. The sweep speed was 1.25nsec/mm resulting in a temporal resolution of approximately 0.25nsec. Figure 9 shows detailed time histories of the 154Å and 162Å emission taken with 12J of laser energy. The emission had a total duration of 6nsec.

Data Analysis

There are some unexpected features to the data in Figs 5-8. First of all, every ALX and ALXI line observed, without exception, showed a non-linear

increase with length. In general the gain coefficient depends on the factors shown in equation 2:

$$G = \frac{1}{8\pi c} \frac{\lambda^4}{\Delta\lambda} g_i A_{ik} \left\{ \frac{N_i}{g_i} - \frac{N_k}{g_k} \right\} \quad (2).$$

Here G is the gain coefficient, and λ the wavelength. g is the statistical weight, A_{ik} the radiative transition probability and N the population of the upper level i and lower level k . The highest gain was expected on the 3-4 transition with the largest gA value (3d-4f at 154Å), however the data shows high gain on all the ALXI and ALX lines observed, similarly to reference 8. Particularly surprising was the strong increase apparent on the ALXI 141Å line, which has a gA value much lower than the 150Å and 154Å transitions. The time history observed with the streak camera showed no difference between the time evolution at 154Å and the continuum background at 162Å (Figure 9). Another unexpected feature is the large rise in the background continuum emission, from 5-10 counts at 2mm to ~200 counts at 10mm. These features raised concerns about the homogeneity of the plasma along its length. Specifically, were the level populations in the region of the 2mm plasma viewed by the spectrometer identical to the conditions in the 10 mm section? As shown in Fig. 4, the 2, 6 and 10mm sections shared a common boundary on the spectrometer end of the target wheel. To test if the plasma was homogeneous a target was built with the 2mm sections on both ends of the target and the 6mm section on the end of the target away from the spectrometer. First the conditions were arranged so as to reproduce the previous 10mm spectra and then the emission from the two 2mm sections at each end of the target was compared. It was immediately apparent that there

was a large difference in intensity between the 2mm section at the spectrometer end and the 2mm section at the opposite end. Taking the average of the 2mm results, the best fit to the data was now a linear increase in intensity with length as shown in Fig. 10. The reason for the non-uniformity lay in a small angle between the target surface and the region viewed by the spectrometer (Fig. 11), possibly caused by refraction. To verify this, the target was rotated about a vertical axis to change the position of the plasma generated by the two 2mm sections with respect to the region viewed by the spectrometer. With a 2° rotation the AlXI 154Å emission from the two ends became equal. In this configuration however the length dependence of the emission was linear. In conclusion; the non-linear increase in Figs 5-8 was caused by geometrical effects and *not* by stimulated emission.

As noted before the measurement of an exponential intensity increase with length is commonly regarded as conclusive evidence for gain (see for instance ref 8). However in view of the above results it is clear that while this may be an encouraging sign of gain it is by no means sufficient proof that gain is present. As was done in some earlier works (for example references 1, 4, 7, 11), it is critical to monitor the emission from nearby spontaneous emission lines in the same ion, preferably lines with the same lower level as the lasing line, to be assured that one is viewing a homogeneous plasma and that the comparison of plasmas of differing lengths is a valid. This is particularly important for measurements of low gain lengths, $GL \leq 4$, where the enhancement of stimulated as compared to spontaneous emission is less than an order of magnitude.

Acknowledgements

We would like to thank E Valeo for assistance with the gain fitting computer program and J Schwarzmann for the target fabrication and G. Howe for assistance with the streak camera. We would also like to acknowledge N. M. Ceglio, D. P. Gaines, G. L. Howe, and E. J. Utterback of the LLNL Advanced X-ray Optics Program for providing TGSS for time resolved spectral measurements. This work was supported by the U.S. Department of Energy, Advanced Energy Projects of Basic Energy Sciences.

Figure Captions

- Fig. 1 The rotatable target system.
- Fig. 2 Spectra obtained with 6J laser energy from carbon plasmas of length: (a) 1mm, (b) 2.5mm and (c) 4.5 mm .
- Fig. 3 Intensities of the CVI 182Å and CVI 135Å lines versus plasma length and (dashed line) a least squares fit to the gain equation (eqn. 1) with a gain of 4.5 cm⁻¹ for the 132Å line.
- Fig. 4 Improved experimental set-up for gain measurements showing the range of angular adjustments available.
- Fig. 5 Aluminum spectra obtained at 6J laser energy with target lengths 2mm and 10mm.
- Fig. 6 Dependence of the AlXI 154Å and AlX 177Å axial line intensity on length. The line represents a fit of the experimental points to the theoretical gain equation (eqn. 1 in the text).
- Fig. 7 Spectra obtained at 12J laser energy with target lengths 2mm and 10mm. Note the x10 scale change from the 2mm to 10mm graph.
- Fig. 8 Dependence of the AlXI 141Å, 150Å, 154Å and AlX 177Å axial line intensity on length. The line represents a theoretical fit of the experimental points to the gain equation (eqn. 1 in the text).
- Fig. 9 Detailed time histories of (a) 154Å and (b) 162Å emission taken with 12J of laser energy. The fluctuations are caused by film grain.

Fig. 10 (a) data showing the 154\AA intensity variation with length but in this case including 2mm sections from both ends of the target. The 6mm data was from a section at the opposite end of the target to the data in Figs 5-8. (b) as above but with the target rotated by 2° .

Fig. 11 Illustration of the effect of a small angle between the plasma and the region viewed by the spectrometer. The comparison of plasmas of differing lengths cannot be used for measurements of gain in this case.

References

- 1 C.H. Skinner, D.S. DiCicco, D Kim, R.J. Rosser, S. Suckewer, A.P. Gupta, and J.G. Hirschberg *J. Micros.* 1989 in press.
- 2 D. L. Matthews, P. L. Hagelstein, M. D. Rosen, M.J. Eckart, N.M. Ceglio, A. U. Hazi, J. Medeck, B. J. MacGowan, J. E. Trebes, B. L. Whitten, E. M. Campbell, C. W. Hatcher, A. M. Hawryluk, R. L. Kaufman, L. D. Pleasance, G. Rambach, J. Scofield, G. Stone, and T. A. Weaver, *Phys. Rev. Lett.* **54**, 110, (1985) and C.J.Keane, N.M.Ceglio, B. J. MacGowan, D. L. Matthews, D. G. Nilson, J. E. Trebes, and D. A. Wilson UCRL Preprint 100546, Feb 1989 submitted to *J. Phys B*.
- 3 S. Suckewer, C. H. Skinner, D. Kim, E. Valeo, D. Voorhees, and A. Wouters *Phys Rev. Lett.* **57**, 1004, (1986).
- 4 D.Kim, C.H. Skinner, G. Umesh, and S. Suckewer *Optics Letters*, **14**, 665-667, 1989.
- 5 S. Suckewer X-ray laser Related Experiments and Theory at Princeton *OSA Proceedings on Short Wavelength Coherent Radiation: Generation and Applications* **2**, 36, (1988).
- 6 based on the RNLIN subroutine in the IMSL STAT/LIBRARY p239.
- 7 G. Jamelot, P. Jaeglé, A. Carillon, F. Gadi, B. Gauthé, H. Guennou, A. Klisnick, C. Möller, and A. Sureau, *I.E.E.E. Trans on Plasma Science*, **16**, 497, (1988).
- 8 T. Hara, K. Ando, N. Kusakbe, H. Yashiro, and Y. Aoyagi *Jpn. J of Appl. Phys.* **6**, 1010-1012, (1989).

-
- 9 J.L.Schwob, A. Wouters, and S. Suckewer, *Rev. Sci. Instrum.* **58**, 1601, (1987).
- 10 N.M.Ceglio in *Laser Interaction and Related Phenomena*, H. Hora and G. Miley,eds., **7**, 39, Plenum Press, New York, 1986. In the present work the TGSS was used without the imaging mirror described in this reference.
- 11 S. Suckewer, C. H. Skinner, D. Kim, E. Vaico, D. Voorhees, and A. Wouters *Phys Rev. Lett.* **57**, 1004, (1986) and D. Kim, C. H. Skinner, A. Wouters, E. Vaico, D. Voorhees and S. Suckewer *J. Opt. Soc. Am B* **6**, 115, 1989.

#89X0674

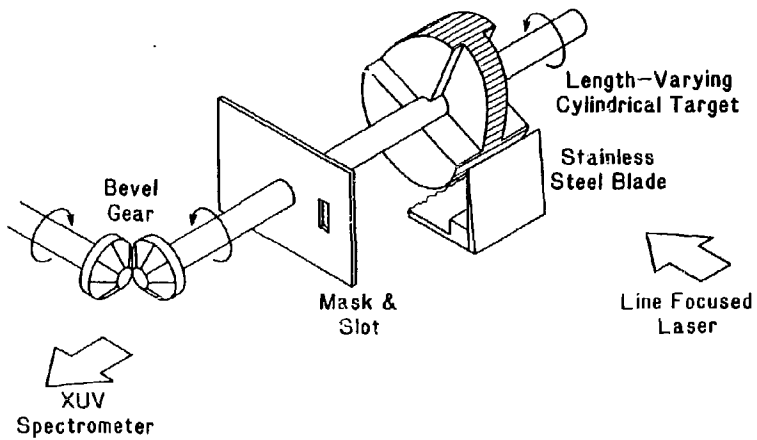


Fig. 1

#89X0675

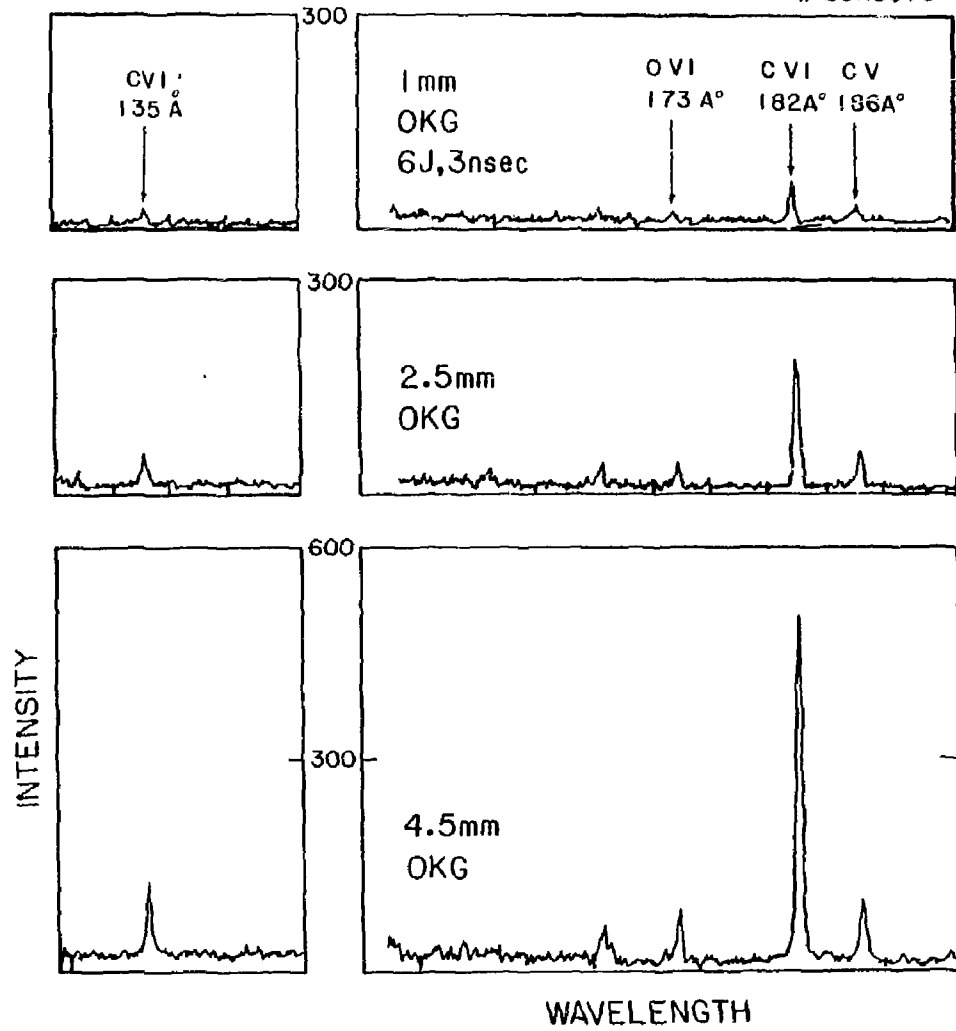


Fig. 2

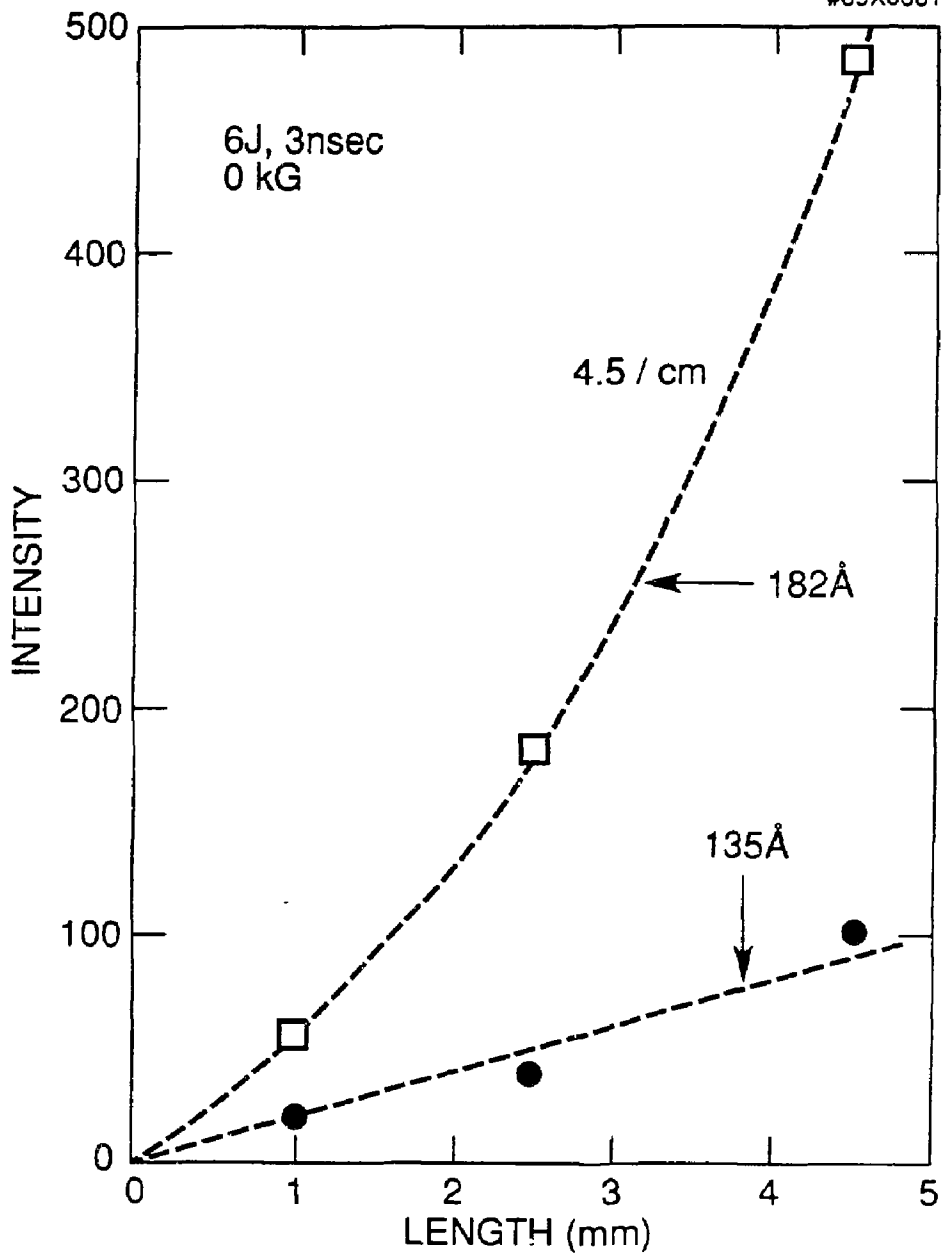
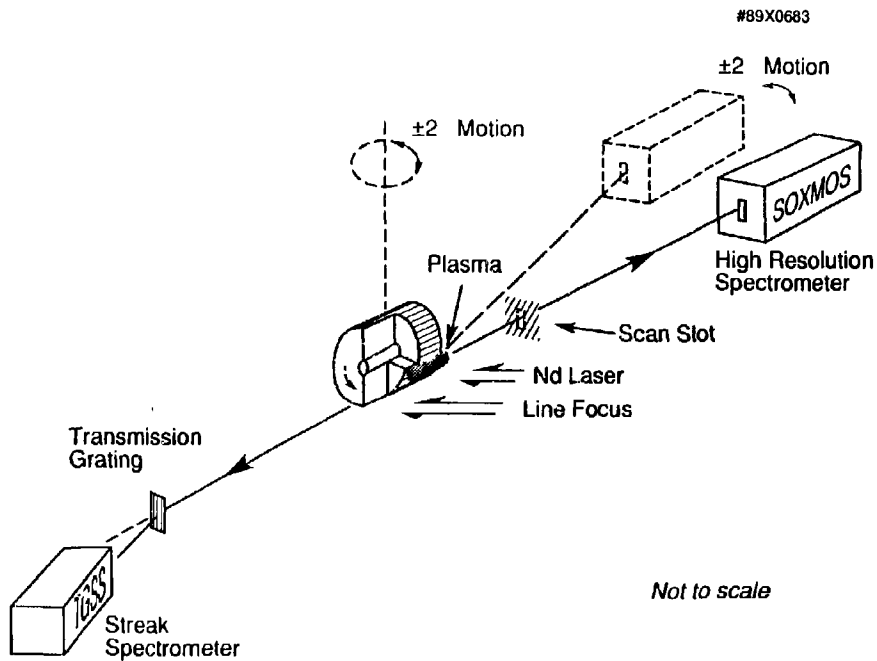


Fig- 3

Fig. 4
17



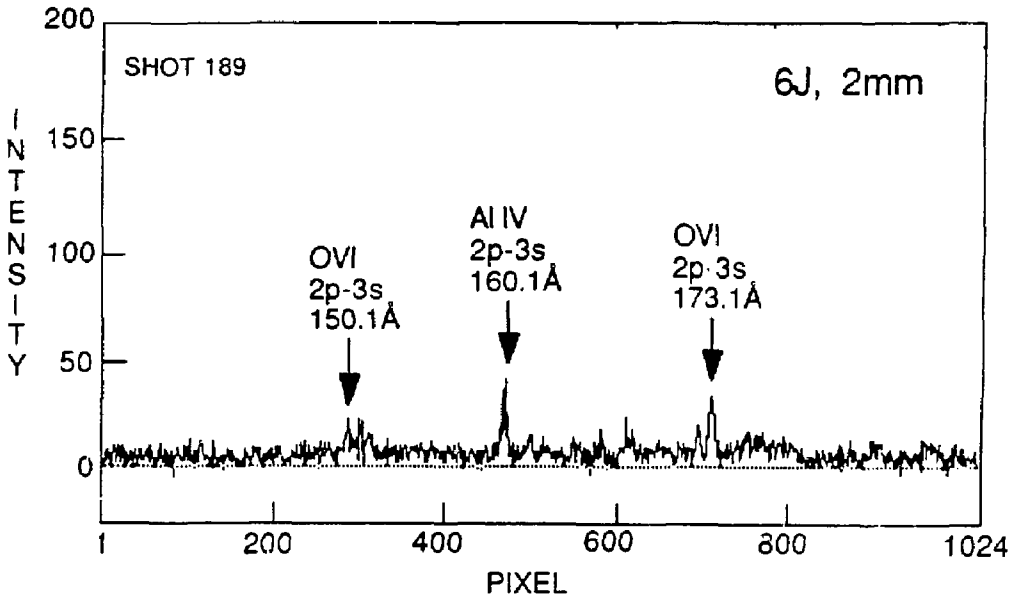
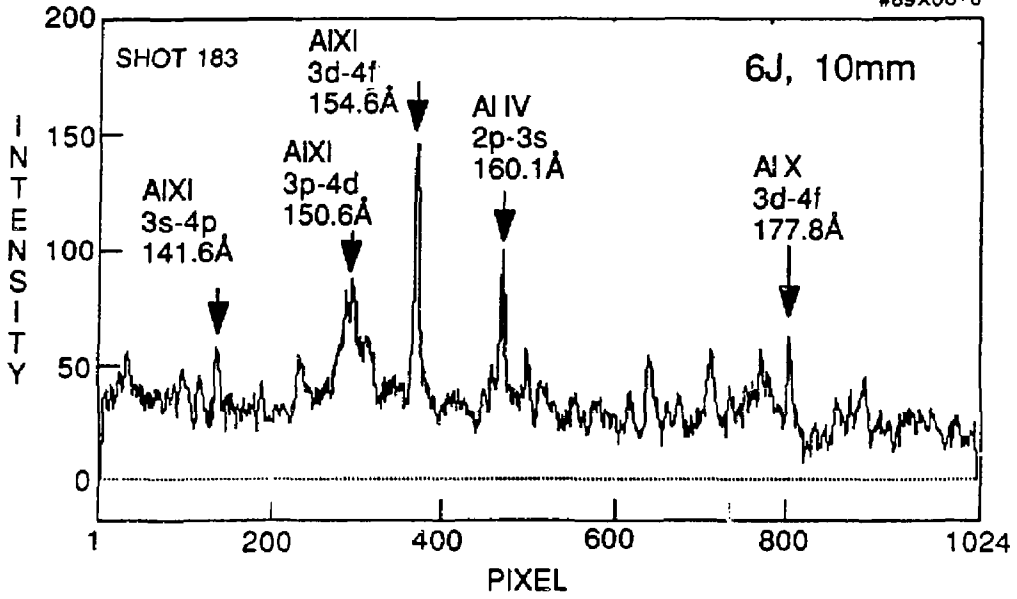


Fig. 5

#89X0679

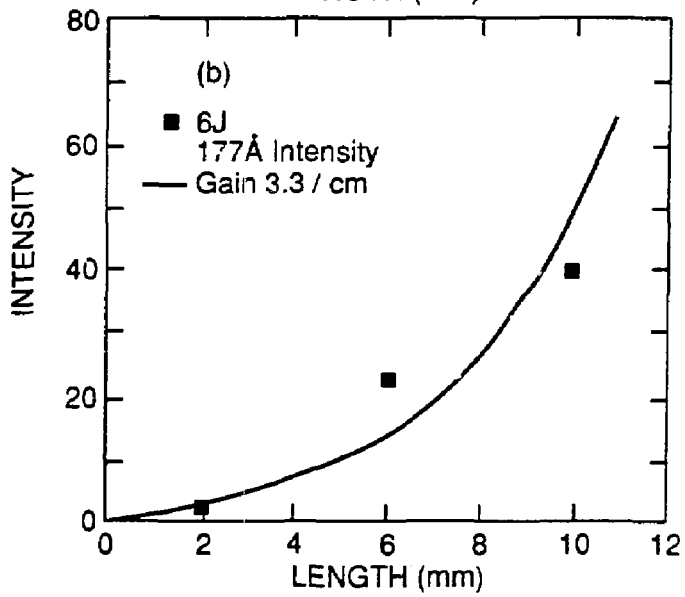
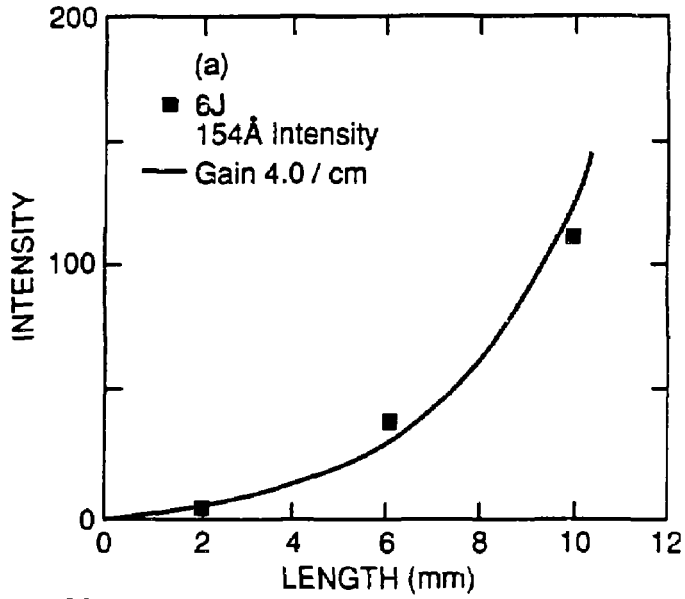


Fig. 6
19

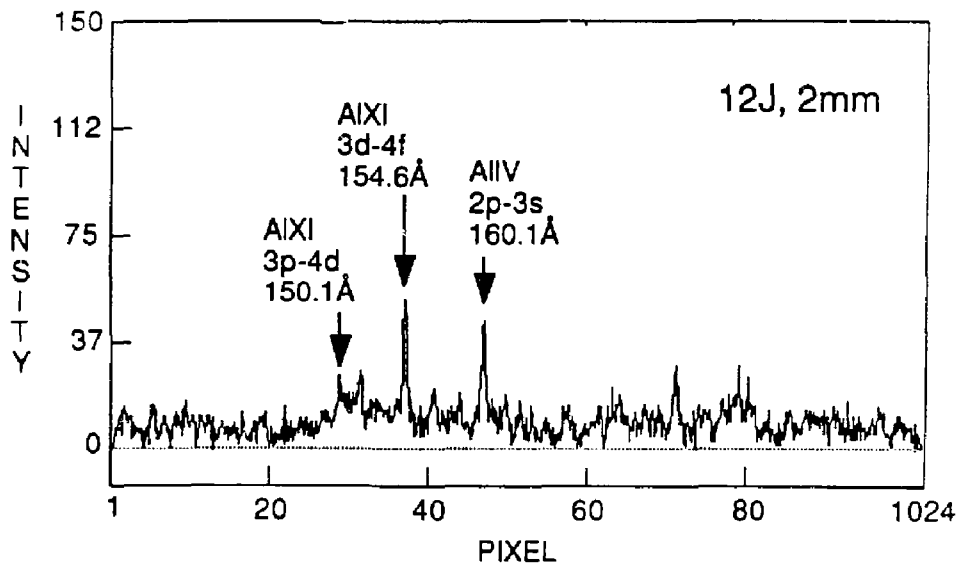
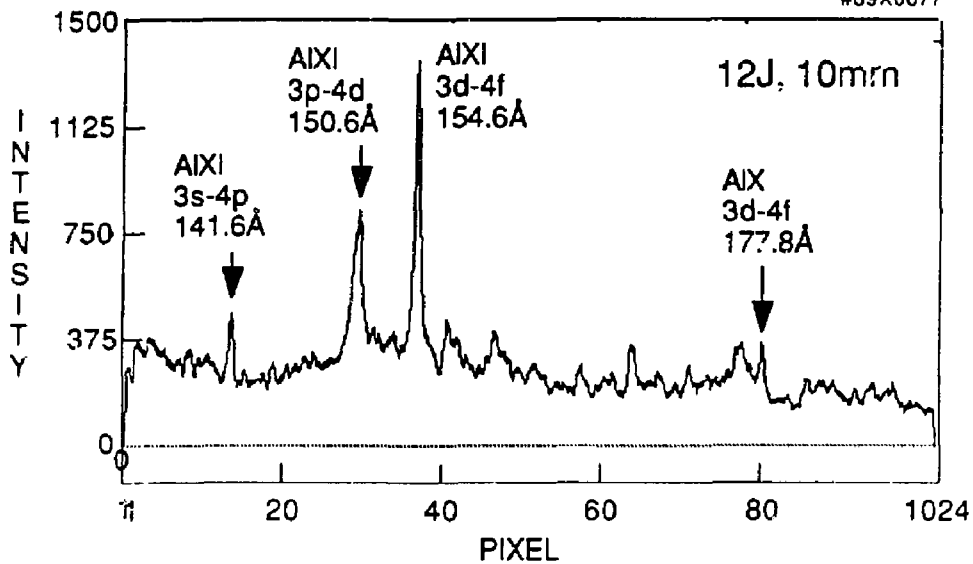


Fig. 7

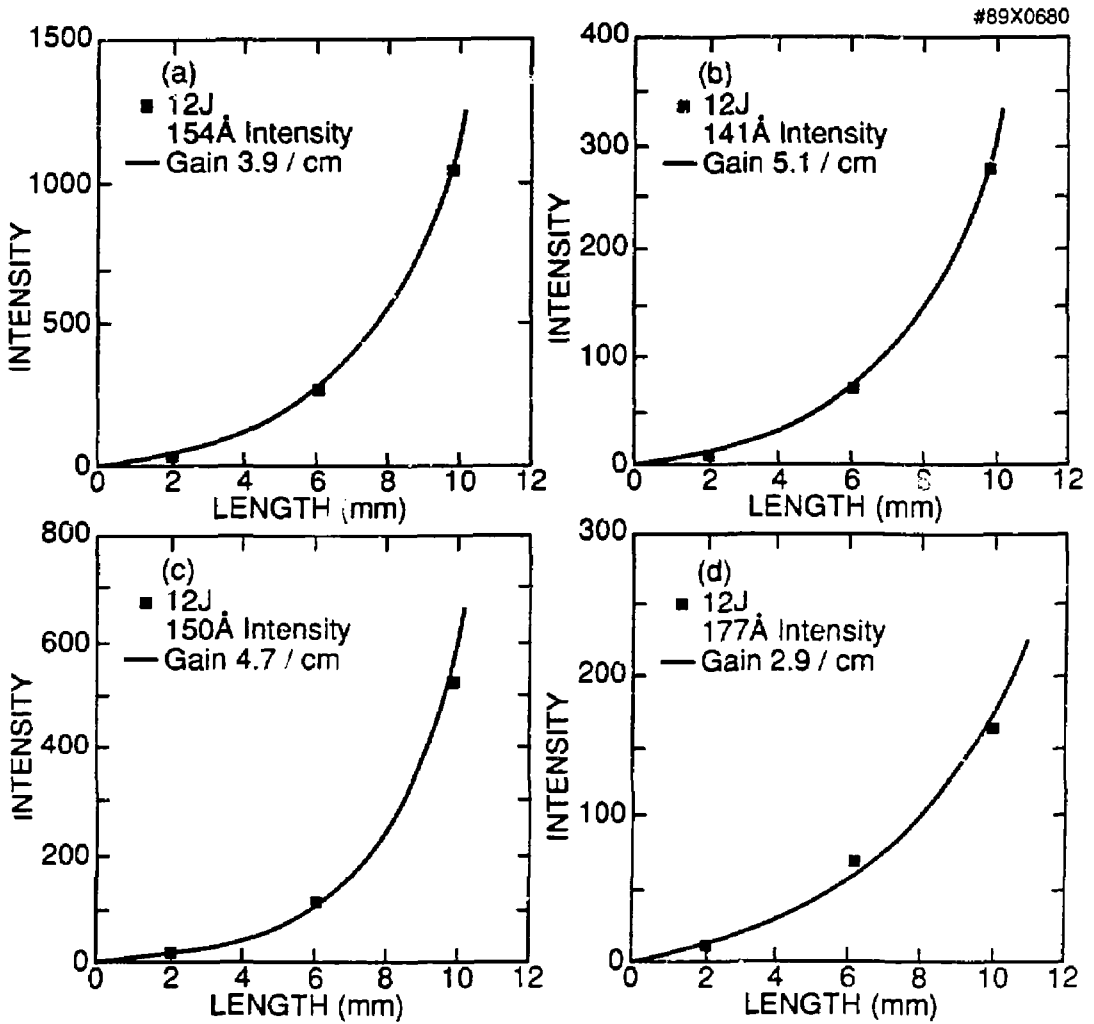


Fig. 8

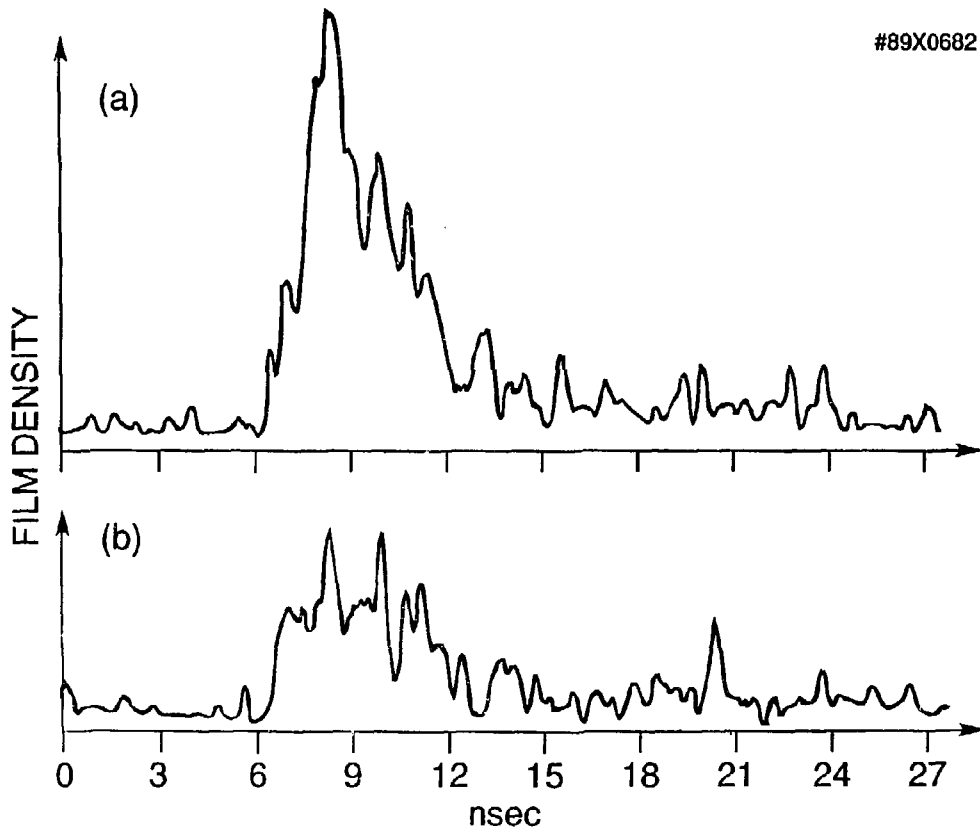


Fig. 9

#89X0678

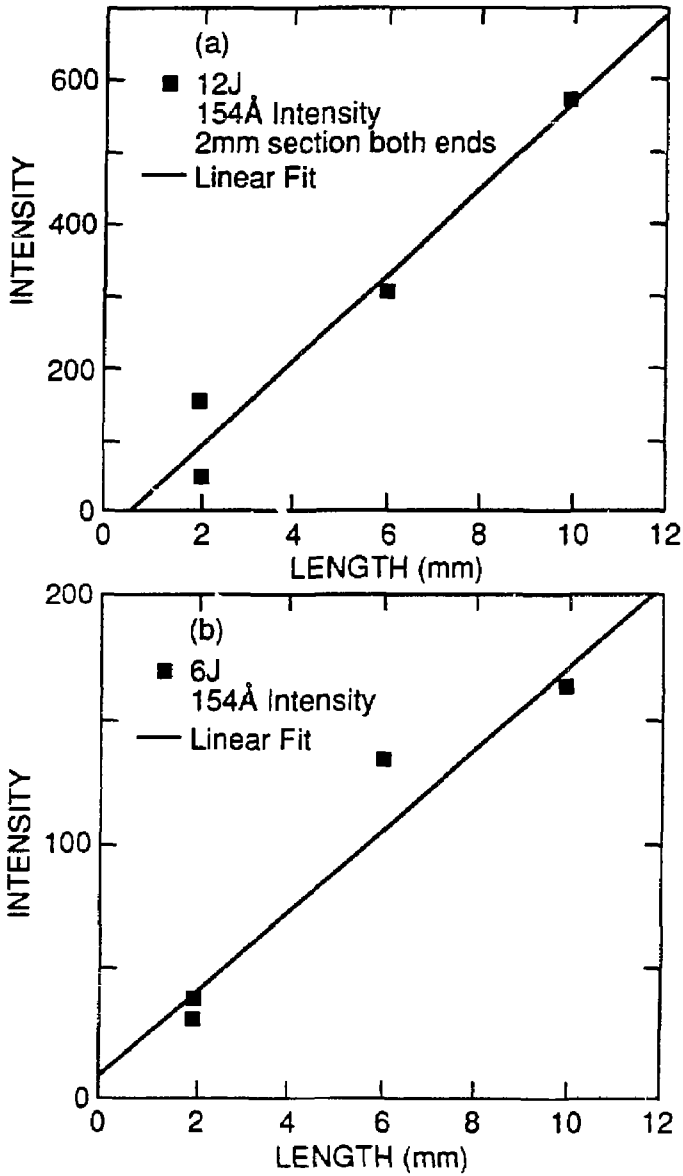


Fig. 10

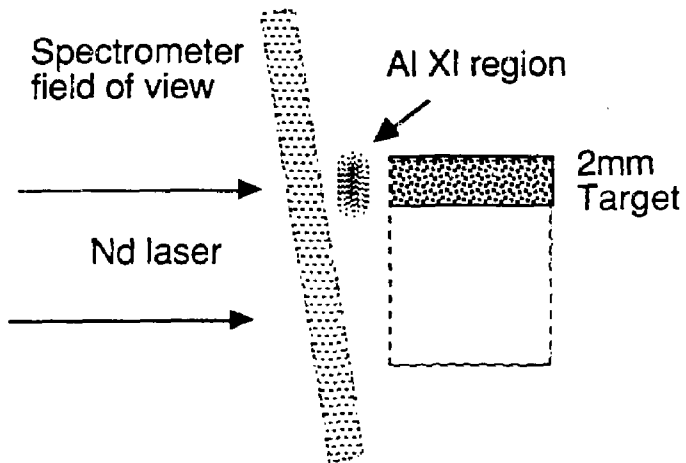
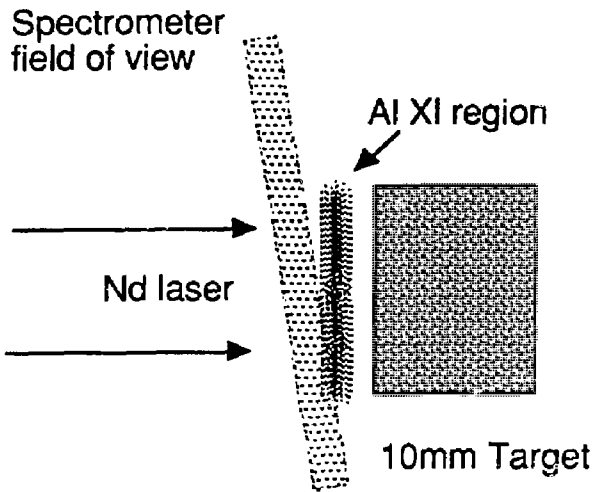


Fig. 11
24